

# Crossed cerebellar diaschisis in acute ischemic stroke: a study with serial SPECT and MRI

Yawu Liu<sup>1</sup>, Jari O Karonen<sup>2</sup>, Juho Nuutinen<sup>3</sup>, Esko Vanninen<sup>4</sup>, Jyrki T Kuikka<sup>4,5</sup> and Ritva L Vanninen<sup>1</sup>

<sup>1</sup>Department of Clinical Radiology, Kuopio University Hospital, Kuopio University, Kuopio, Finland;

<sup>2</sup>Department of Radiology, Mikkeli Central Hospital, Mikkeli, Finland; <sup>3</sup>Department of Neurology, Kuopio University Hospital, Kuopio University, Kuopio, Finland; <sup>4</sup>Department of Clinical Physiology and Nuclear Medicine, Kuopio University Hospital, Kuopio University, Kuopio, Finland; <sup>5</sup>Niuvanniemi Hospital, Kuopio, Finland

**This study evaluated the relationship between crossed cerebellar diaschisis (CCD) and (1) lesion volume and location in the acute phase and 1 week after stroke onset and (2) clinical outcome. Twenty-two patients with cerebral ischemic stroke underwent single-photon emission computed tomography (SPECT) and magnetic resonance imaging (MRI) within 48 h and on day 8 from onset. Interhemispheric asymmetric indices (AI) on SPECT were calculated for medial, intermediate, and lateral zones of the cerebellum. Lesion volumes and locations were obtained from diffusion-weighted MRI. Neurological status and 3-month clinical outcome were evaluated. Within 48 h, lesion locations in the temporal association cortex and pyramidal tract of the corona radiata were independent determinants for the AI of the medial zone ( $R^2 = 0.439$ ). Lesion locations in the primary, premotor, and supplementary motor cortices, primary somatosensory cortex, and anterior part of the posterior limb of the internal capsule were determinants for the AI of the intermediate zone ( $R^2 = 0.785$ ). Lesions in the primary motor cortex, premotor, and supplementary motor cortices and in the genu of the internal capsule were determinants for the AI of the lateral zone ( $R^2 = 0.746$ ). On day 8, the associations were decreased. The AIs of the intermediate and lateral zones and lesion location in the parietal association cortex were independently associated with the 3-month clinical outcome ( $R^2 > 0.555$ ). Acute CCD is a result of functional deafference, while in the subacute phase, transneuronal degeneration might contribute to CCD. CCD in the intermediate and lateral zones is a better indicator than that in the medial zone.**

*Journal of Cerebral Blood Flow & Metabolism* (2007) 27, 1724–1732; doi:10.1038/sj.jcbfm.9600467; published online 21 February 2007

**Keywords:** acute; crossed cerebellar diaschisis; diffusion-weighted imaging; human; magnetic resonance imaging; stroke

## Introduction

Crossed cerebellar diaschisis (CCD) is matched hypoperfusion and hypometabolism in the cerebellum due to the remote effect of a contralateral supratentorial lesion. This phenomenon was first discovered in human supratentorial infarction by Baron *et al* (1980), and was first reviewed by Feeney and Baron (1986). The most likely mechanism is loss

of afferent stimuli due to the damage of cerebrocerebellar pathways. It is believed that CCD happens immediately after loss of afferent stimulate (Gold and Lauritzen, 2002). Evidence has shown that the presence of CCD at the acute stage predicts unfavorable clinical outcomes (De Reuck *et al*, 1997; Sobesky *et al*, 2005; Takasawa *et al*, 2002).

Some studies have been carried out in humans with single-photon emission computed tomography (SPECT) and positron emission tomography (PET) to study CCD (De Reuck *et al*, 1997; Kamouchi *et al*, 2004; Kim *et al*, 1997; Komaba *et al*, 2004; Pantano *et al*, 1986; Yamauchi *et al*, 1999), but the relationship between the severity of CCD and the infarct volume is still controversial. Few studies have investigated the relationship between the infarct location and CCD in humans by means of a combination of magnetic resonance imaging (MRI)

Correspondence: Dr Y Liu, Department of Clinical Radiology, Kuopio University Hospital, Kuopio University, FIN-70210, Kuopio, Finland.

E-mail: Yawu.Liu@kuh.fi

This work is supported by EVO funding of Kuopio University Hospital, NEKU2, and EU Regional Funding Project (70068/05). Received 10 November 2006; revised 3 January 2007; accepted 8 January 2007; published online 21 February 2007

and SPECT or PET. One of the disadvantages of SPECT and PET is that it is very difficult to accurately localize the malfunctioning ischemic brain area because of the low resolution.

MRI has a much higher resolution than SPECT or PET. The diffusion-weighted MRI (DWI) is one of the most sensitive tools to monitor the neural function in clinical practice. Diffusion-weighted magnetic resonance imaging can detect the cellular edema owing to the failure of the ionic pump on the cellular membrane minutes after the occlusion of the middle cerebral artery (Moseley *et al*, 1990). In this study, we used SPECT to detect the CCD and DWI to detect malfunctioning ischemic brain tissue to evaluate (1) the relationship between CCD defined with SPECT and ischemic volumes measured on DWI, (2) the relationship between the CCD and DWI lesion locations, (3) the temporal evolution of CCD during the first week in patients with first-ever supratentorial ischemic stroke, and finally (4) the clinical significance of CCD on the outcome of ischemic stroke.

## Materials and methods

Twenty-two patients (8 women and 14 men) with their first-ever acute ischemic stroke were selected prospectively. The inclusion criteria were as follows: (1) the patient had symptoms and signs indicative of acute hemispheric stroke, and computed tomography did not reveal hemorrhage or other nonischemic causes for symptoms, (2) the first MRI and SPECT could be performed within 48 h of the onset of symptoms, (3) the patient had no general contraindications for MRI (e.g., cardiac pacemaker, ferromagnetic aneurysm clips, and infusion devices), and (4) the patients were likely to undergo the follow-up MRI and SPECT examinations 1 week later (day 8).

The mean age (mean  $\pm$  s.d.) of the patients was  $70 \pm 9$  years. The time that the patient was last known to be healthy was recorded as the time of stroke onset. The median of time delay from the onset of symptoms to the first MR examination was 13 h (range = 3.5 to 41.5 h) and to SPECT hours (range = 4.3 to 42.8 h). Patients were treated with aspirin and/or dipyridamole, or anticoagulation, and all received standard supportive therapy for ischemic stroke. None of the patients received thrombolytic or experimental neuroprotective agents. To determine the normal range of asymmetry index (AI), 10 healthy volunteers ( $39 \pm 9$  years) were imaged with SPECT.

The study design was approved by the Ethics Committee of our institute. Informed consent was obtained from the patient or the patient's relative.

### Magnetic Resonance Imaging

All MR imaging studies were performed with a 1.5 T whole body scanner capable of echo planar imaging (Magnetom Vision, Siemens Medical Systems, Erlangen, Germany) using a head coil. The patient's head was fixed

with standard restraints used in routine clinical MR imaging. Each MR imaging examination consisted of DWI, perfusion-weighted imaging, two-dimensional phase-contrast MR angiography (2D-PC-MRA) of the circle of Willis, T2-, and proton density (PD)-weighted axial fast spin-echo imaging, and pre and after contrast T1-weighted axial spin-echo imaging. Only the DWI and T2-weighted MRI data are presented in this study.

Diffusion-weighted magnetic resonance imaging was performed with a single-shot echo planar spin-echo sequence (repetition time, 4000 ms and echo time, 103 ms). Other imaging parameters were: slice thickness, 5 mm; interslice gap, 1.5 mm; field of view, 260 mm; matrix size,  $96 \times 128$  interpolated to  $256 \times 256$ ; and total acquisition time, 20 s. Nineteen axial slices parallel to the orbitomeatal line were imaged, covering all supra- and subtentorial brain tissue. Four images per slice were obtained: one T2-weighted image without diffusion weighting ( $b$ -value =  $0 \text{ s/mm}^2$ ) and three diffusion weighted images with orthogonally applied diffusion gradients ( $b$ -value =  $1000 \text{ s/mm}^2$ ). To avoid the effects of diffusion anisotropy, isotropic diffusion-weighted images were calculated as the geometric mean of the three diffusion-weighted images on a voxel by voxel basis.

### Single-Photon Emission Computed Tomography Imaging

Technetium-99m ethyl cysteinate dimer ( $^{99m}\text{Tc}$ -ECD) was used as the tracer. A dose of 550 to 720 MBq, varying according to the body weight of the patient, was injected into an antecubital vein within 2 h of the perfusion-weighted imaging in 20 patients, and within 2.9 to 3.4 h of perfusion-weighted imaging in two patients. Within 60 mins after the injection, high-resolution SPECT acquisition was performed with a gamma camera equipped with fan-beam collimators (MultiSPECT 3, Siemens Medical Systems Inc., Hoffman Estates, IL, USA). A full  $360^\circ$  rotation was acquired (40 views/detector, each for 35 secs). The matrix size was  $128 \times 128$ , and the imaging resolution was 8 to 9 mm. Contiguous 6.5-mm-thick axial slices aligned parallel with the orbitomeatal line were reconstructed by filtered backprojection and a uniform attenuation correction was performed.

### Assessment of Neurological and Functional Status

The National Institute of Health Stroke Scale (NIHSS) was used to evaluate the neurological and functional status before each MRI and at 3 months after the stroke. In addition, the patients' ability to perform daily activities was assessed according to the modified Rankin scale (mRS) 3 months after the stroke.

### Regional Analysis

First, the DWI lesions were localized by a radiologist with 11 years of experience in MRI. Then, based on the radiologist's functional and anatomical knowledge, the location of the DWI lesion was classified according to 12

main functional or anatomical areas (Duvernoy, 1991), that is primary motor cortex (precentral gyrus), premotor and supplementary cortex (superior, middle, and inferior frontal gyri, areas 6, 8, 44, and 45), primary somatosensory cortex (postcentral gyrus), secondary somatosensory cortex (parietal operculum of inferior parietal gyrus), parietal association cortex (superior parietal lobule and supramarginal and angular gyri), auditory cortex (transverse and superior temporal gyri), temporal association cortex (middle and inferior temporal gyri and fusiform gyrus), primary visual cortex (cuneus and lingual gyrus), visual association cortex (lateral and superior occipital gyri), limbic system (prefrontal cortex, amygdale, hypothalamus, hippocampus, and parahippocampal gyrus), basal ganglia, and thalamus. The involvement of the pyramidal tract in corona radiata, internal capsule (anterior limb, genu, and posterior limb), and visual radiate was also analyzed. Presence or absence of DWI lesion in each cerebral area and fiber tract were coded as present = 1 and absent = 0.

The total DWI lesion volumes on the initial day and on day 8 MRI were measured from isotropic diffusion-weighted images. Volumes of the lesion were measured by drawing regions of interest (ROIs) around the lesions on the isotropic diffusion-weighted images and by multiplying the lesion area by the slice thickness. The interslice gap was estimated to contain a lesion of the same size as the slice above it, and the lesion inside the gap was included in the volume calculation.

Based on the fiber projection of the cerebral cortex onto the cerebellar deep nuclei, the corpus cerebella can be divided into three longitudinal zones: (1) medial, (2) intermediate and, (3) lateral (Zigmond *et al*, 1999). We measured counts from the three zones (Figure 1) on ipsilateral cerebellar hemisphere as well as on mirrored contralateral hemisphere on four consecutive slices of SPECT images. The cerebellar interhemispheric AI on SPECT was calculated for three zones as below:

$$AI = (ICL - CCL)/(ICL + CCL) \times 100\% \quad (1)$$

where ICL = the total counts of one zone in the ipsilateral cerebellar hemisphere and CCL = the total counts of the corresponding zone in the contralateral cerebellar hemisphere. The AI of each volunteer was also calculated in the same way, but instead of using CCL and ICL, the total counts of the corresponding zone in the right and left cerebellar hemispheres were used. The average AI was then calculated by averaging the AIs from the four slices weighed by their sizes. In volunteers, the 95% confidence interval of AIs of the medial, intermediate, and lateral zones were 4.4% to 3.6%, 3.1% to 2.0%, and 5.8% to 4.6%, respectively. In patients, CCD was considered to be present if the AI of a certain zone was larger than the upper limit of the 95% confidence interval of the AI in the corresponding zone of volunteers.

### Statistical Analysis

The  $\chi^2$  test was used to analyze the difference in frequencies to ascertain the presence of CCD in the three cerebellar zones. The Pearson correlation coefficient (for

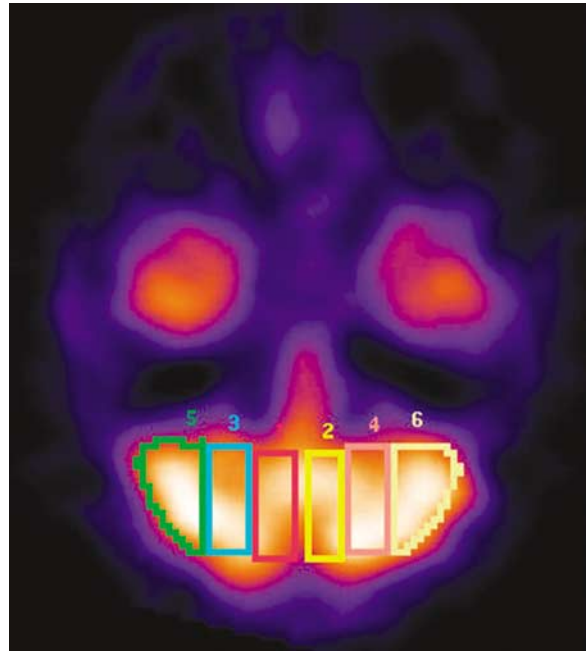


**Figure 1** The ROIs 1 and 2 indicate the medial zones, ROIs 3 and 4 indicate the intermediate zones, and ROIs 5 and 6 indicate the lateral zones.

DWI lesion volume) and Independent Student's *t*-test (for DWI lesion locations) were used to evaluate the association between the AIs and DWI lesion volume and locations. If the DWI lesion volume and locations showed significant association with the AI, then they were further included in a stepwise multivariable linear regression model. In the stepwise multivariable linear regression analysis, the AIs were used as dependent variables and the infarct volumes (continuous variable) and infarct locations (dichotomized variable) were used as independent variables. The same statistical approach was used to evaluate the determinants of the 3-month clinical outcome (modified Rankin scale). The  $P < 0.05$  was considered as statistical significant.

### Results

Within the first 48 h of symptom onset, 2 (9%), 11 (50%), and 7 (32%) of 22 patients showed CCD in the medial, intermediate, and lateral cerebellar zones, respectively. On day 8, there were three, four, and two new patients presenting with CCD in the three respective zones. However, of the patients who showed CCD on initial SPECT, there were also 1, 1, and 2 patients, respectively, whose AIs on day 8 in the three zones decreased to within the upper 95% confidence interval limits of the AIs of normal volunteers. Therefore, on day 8, there were in all 4 (18%), 14 (64%), and 7 (32%) of 22 patients presenting with CCD in the medial, intermediate, and lateral cerebellar zones, respectively (Table 1). The frequencies of CCD significantly differed in the

**Table 1** Clinical characteristics, and lesion volumes and locations of the 22 patients

Patient	Age/sex/ side	DWI lesion volume		DWI lesion location		Initial AI			Day 8 AI			NIHSS			mRS 3-month
		Initial	Day 8	Initial	Day 8	Medial zone	Intermediate zone	Lateral zone	Medial zone	Intermediate zone	Lateral zone	Initial	Day 8	3- month	
1	73/F/R	11.6	72.3	S3, BG, PT, IC2–3	M1–2, S3, L, BG, PT, IC1–3	0.4	1.5	5.7	7.2	7.5	13.1	10	13	7	4
2	56/M/R	35.7	96.7	M1, S1, A2, L, BG, PT, IC2–3	M1, S1, A2, L, BG, PT, IC1–3	3.7	7.2	9.5	3.0	5.6	6.7	16	15	10	3
3	62/M/L	0.9	0.8	PT, IC3*	PT, IC3*	–2.1	–5.7	–1.5	11.9	5.9	–1.6	1	1	8	2
4	81/F/R	3.7	54.2	M1–2, S3, L, BG, PT, IC1, OR	M1–2, S3, L, A2, BG, PT, IC1, OR	0.9	4.1	7.1	0.5	5.3	0.3	13	4	—	6
5	87/M/R	34.5	71.0	S3, V1–2, L, OR	S3, V1–2, L, Th, OR	–3.6	–0.7	0.0	6.5	–3.8	2.6	8	4	2	2
6	74/M/L	32.9	68.0	M1–2, S1, A1, PT	M1–2, S1, A1, PT	2.4	9.1	5.7	2.2	4.9	2.2	12	2	1	1
7	84/F/R	36.5	112.9	M1–2, PT	M1–2, S1, A1, PT	5.2	6.2	5.9	6.6	7.6	7.9	10	15	9	4
8	82/F/L	0.3	0.5	M1	M1	0.0	–1.2	–3.5	–0.3	0.0	–3.9	1	0	0	1
9	60/M/L	1.0	1.0	PT	PT	–0.1	–2.0	0.0	0.9	–3.1	–5.8	1	1	0	0
10	75/M/R	1.6	1.0	PT, IC3*	PT, IC3*	3.5	2.9	0.8	3.1	1.6	1.0	0	0	0	0
11	72/M/R	158.4	379.5	M1–2, S1–3, L, V2, A2, BG, PT, IC1–3	M1–2, S1–3, L, V2, A1–2, BG, PT, IC1– 3	2.6	9.6	13.5	1.5	6.6	10.4	19	21	13	5
12	70/M/L	1.8	1.5	BG, PT, IC3*	BG, PT, IC3*	2.4	1.5	0.7	4.3	3.8	1.6	5	2	0	0
13	53/F/L	92.5	104.4	M1–2, L	M1–2, S1–3, L, A1	0.4	2.9	4.3	0.1	2.0	6.2	7	5	3	3
14	75/F/L	59.0	87.1	M1, S1–3, A1–2, PT	M1, S1–3, A1–2, PT	4.1	3.9	3.9	0.6	4.2	1.5	6	5	4	3
15	75/F/L	6.1	25.8	S1–3, PT, IC3	S1–3, A1, PT, IC3	2.5	3.4	1.3	–2.6	4.1	4.8	14	5	17	4
16	71/M/R	72.3	124.3	M1, S1–3, PT, IC3*	M1, S1–3, PT, IC3*	2.4	4.8	6.0	1.2	4.6	4.6	20	15	10	4
17	68/M/R	6.4	22.4	M1, S1, PT	M1, S1–3, A1, PT	–0.6	5.3	5.0	1.8	–1.8	2.4	5	0	0	0
18	71/F/R	1.8	4.6	Th, IC3*	Th, IC3*	0.2	1.0	6.3	4.1	6.0	11.6	4	4	4	4
19	64/M/L	117.4	187.4	M1–2, S2–3, L, A1– 2, BG, PT, IC1–3	M1–2, S1–3, L, A1– 2, BG, PT, IC1–3	6.4	8.5	12.6	3.4	7.4	8.4	30	22	19	4
20	64/M/L	12.1	5.3	V1, L, Th, IC3*	V1, L, Th, IC3*	1.6	–2.3	–0.4	0.7	3.0	2.8	6	5	2	3
21	67/M/L	68.4	59.2	M2, A1–2, BG	M2, A1–2, BG	–2.0	3.5	2.3	2.3	6.2	3.9	8	4	3	2
22	59/M/R	3.0	10.5	PT	S1, PT, IC3*	0.6	–0.9	–0.1	0.5	2.0	0.3	4	0	1	0

A1 auditory cortex, A2 temporal association cortex, BG basal ganglia, IC1 anterior limb, IC2 genu, IC3 posterior limb of internal capsule, L limbic system, M1 primary motor cortex, M2 premotor and supplementary motor cortex, mRS modified Rankin scale, NIHSS National institute of health stroke scale, OR optical radiate, PT pyramidal tract in corona radiata, S1 primary somatosensory cortex, S2 secondary somatosensory, S3 parietal association cortex, Th thalamus, V1 primary visual cortex, and V2 visual association cortex. \* indicates lesion involved posterior part of posterior limb of internal capsule.

three zones (within the first 48 h,  $P=0.013$ ; on day 8,  $P=0.006$ ).

The total lesion volume was  $34 \pm 43$  mL on initial DWI. The DWI lesion volume increased during the follow-up period to  $68 \pm 86$  mL on day 8 (Table 1). The initial DWI lesion volume was significantly associated with the AIs of the intermediate and lateral zones ( $r=0.620$ ,  $P=0.002$ ;  $r=0.690$ ,  $P<0.001$ , respectively), but not with the AI of the medial zone ( $r=0.332$ ,  $P=0.131$ ). On day 8, the DWI lesion volume was significantly associated with the AI of the lateral zone ( $r=0.543$ ,  $P=0.009$ ), but not with the AIs of the medial and intermediate zones ( $r=-0.046$ ,  $P=0.839$ ;  $r=0.405$ ,  $P=0.061$ , respectively).

In univariate analyses, the AI of the medial zone was associated with DWI lesion locations in the primary motor cortex, auditory cortex, temporal association cortex, and pyramidal tract in the corona radiata within 48 h of symptoms onset. The AI of the intermediate zone was associated with DWI lesion locations in the primary, premotor, and supplementary motor cortices, primary and secondary somatosensory cortices, auditory cortex, temporal association cortex, anterior limb, genu, and anterior part of the posterior limb of the internal capsule. The AI of the lateral zone was associated with DWI lesion locations in primary, premotor, and supplementary motor cortices, temporal association cortex, basal ganglia, and anterior limb, genu, and anterior part of the posterior limb of the internal capsule (Table 2).

However, when the above variables were fed into the stepwise multivariable linear regression model, only the AI of the medial zone was independently associated with DWI lesion locations in the temporal association cortex (standardized coefficient  $\beta=0.443$ ,  $P=0.023$ ) and pyramidal tract in corona radiata ( $\beta=0.381$ ,  $P=0.047$ ;  $R^2=0.439$ ). The AI of the intermediate zone was independently associated with DWI lesion locations in the primary ( $\beta=0.332$ ,  $P=0.029$ ), premotor and supplementary motor cortices ( $\beta=0.382$ ,  $P=0.009$ ), primary somatosensory cortex ( $\beta=0.349$ ,  $P=0.013$ ), and anterior part of the

posterior limb of the internal capsule ( $\beta=0.281$ ,  $P=0.028$ ;  $R^2=0.785$ ). The AI of the lateral zone was independently associated with DWI lesion locations in primary motor cortex ( $\beta=0.297$ ,  $P=0.045$ ), premotor and supplementary cortices ( $\beta=0.299$ ,  $P=0.042$ ), and genu of the internal capsule ( $\beta=0.580$ ,  $P<0.001$ ;  $R^2=0.746$ ) (Figures 2 and 3).

On day 8, the AI of the medial zone was not associated with either DWI lesion volume or DWI lesion locations in univariate analyses. In contrast, the AI of the intermediate zone was associated with DWI lesion locations in premotor and supplementary motor cortex, temporal association cortex, basal ganglia, and anterior limb, genu, and anterior part of the posterior limb of the internal capsule. The AI of the lateral zone was associated with DWI lesion volume, DWI lesions in premotor and supplementary motor cortex, limbic system, and anterior limb, genu, and anterior part of the posterior limb of the internal capsule (Table 2).

When these variables were fed into the stepwise multivariable linear regression model, however, the AI of the intermediate zone was significantly associated with only the DWI lesion location in the premotor and supplementary motor cortex ( $\beta=0.540$ ,  $P=0.009$ ;  $R^2=0.292$ ). The AI of the lateral zone was significantly associated with only the DWI lesion location in the genu of the internal capsule ( $\beta=0.607$ ,  $P=0.003$ ;  $R^2=0.369$ ) (Figures 2 and 3).

The correlation between AIs and NIHSS or mRS is summarized in Table 3. The AIs of the three zones on initial SPECT were significantly associated with NIHSS in the acute phase and on day 8 after stroke onset and at 3 months ( $r \geq 0.497$ ,  $P \leq 0.040$ ), but only the AI of the lateral zone was significantly associated with mRS at 3 months ( $r=0.617$ ,  $P=0.002$ ). The AIs of the intermediate and lateral zones on day 8 were significantly associated with NIHSS and mRS at each time point ( $r \geq 0.509$ ,  $P \leq 0.016$ ), but the AI of medial zone on day 8 was not ( $P \geq 0.570$ ). The AI of the intermediate zone on day 8 correlated best with 3-month NIHSS ( $r=0.604$ ,  $P=0.004$ ) and mRS ( $r=0.629$ ,  $P=0.002$ ).

**Table 2** Association (Independent Student's *t*-test) between cerebellar interhemispheric asymmetry index and infarction locations

<i>P</i> value	Medial zone AI	Intermediate zone AI	Lateral zone AI
<i>Within 48 h</i>			
<0.05	M1, A1, A2, PT	M1, M2, S1, S2, A1, A2, IC1, IC2, IC3 <sup>1</sup>	M1, M2, A2, BG, IC1, IC2, IC3 <sup>1</sup>
≥0.05	M2, S1, S2, S3, V1, V2, L, BG, Tha, IC1, IC2, IC3 <sup>1</sup> , C3 <sup>2</sup> , OR	S3, V1, V2, L, BG, Tha, PT, IC3 <sup>2</sup> , OR	S1, S2, S3, V1, V2, A1, L, Tha, PT, IC3 <sup>2</sup> , OR
<i>Day 8</i>			
<0.05	—	M2, A2, BG, IC1, IC2, IC3 <sup>1</sup>	M2, L, IC1, IC2, IC3 <sup>1</sup>
≥0.05	M1, M2, S1, S2, S3, V1, V2, A1, A2, L, BG, Tha, PT, IC1, IC2, IC3 <sup>1</sup> , IC3 <sup>2</sup> , OR	M1, S1, S2, S3, V1, V2, A1, L, Tha, PT, IC3 <sup>2</sup> , OR	M1, S1, S2, S3, V1, V2, A1, A2, BG, Tha, PT, IC3 <sup>2</sup> , OR

A1 auditory cortex, A2 temporal association cortex, BG basal ganglia, IC1 anterior limb, IC2 genu, IC3<sup>1</sup> and IC3<sup>2</sup> anterior and posterior part of posterior limb of internal capsule, respectively, L limbic system, M1 primary motor cortex, M2 premotor and supplementary motor cortex, OR optical radiate, PT pyramidal tract in corona radiata, S1 primary somatosensory cortex, S2 secondary somatosensory, S3 parietal association cortex, Th thalamus, V1 primary visual cortex, V2 visual association cortex.

In univariate analyses, within 48 h of symptom onset, the DWI lesion locations in the parietal association cortex, limbic system, anterior limb of internal capsule, and anterior part of the posterior limb of the internal capsule were significantly associated with the 3-month mRS ( $P < 0.05$ ); on day 8, the DWI lesion locations in the premotor and supplementary motor cortex, parietal association

cortex, temporal association cortex, limbic system, anterior limb of internal capsule, and anterior part of posterior limb of internal capsule were significantly associated with the 3-month mRS ( $P < 0.05$ ). When these variables and AIs were fed into the stepwise multivariable linear regression model, during the first 48 h of onset, only the DWI lesion location in the parietal association cortex and the AI of the lateral zone were independently associated with the 3-month mRS ( $R^2 = 0.555$ ); on day 8, the DWI lesion location in the parietal association cortex and the AI of the intermediate zone were independently associated with 3-month mRS ( $R^2 = 0.660$ ).

## Discussion

In our study, within the first week of the onset of supratentorial stroke, the DWI lesions in primary, premotor, and supplementary motor cortices, primary and secondary somatosensory cortices, auditory cortex, temporal association cortex, basal ganglia and limbic system, and their fiber pathways were clearly associated with the AIs in the three cerebellar zones, supporting the assumption that a cerebro-cerebellar fiber projection fashion similar to that studied in nonhuman primates exists also in humans. By using a combination of anatomical tract tracing and physiological characterization of neuronal receptive fields in nonhuman primates, the cortico-ponto-cerebellar and cortico-olivo-cerebellar pathways have been explored. These pathways carry associative, paralimbic, sensory, and motor information from the cerebral cortex to the neurons in the ventral pons and inferior olive. The axons of these neurons reach the cerebellar cortex in three main longitudinal zones via the pontocerebellar pathway and climbing fiber system (Allen and Tsukahara, 1974; Brodal, 1972; Schmahmann and Pandya, 1997; Zigmond *et al*, 1999).

The fibers from cortico-ponto-cerebellar and cortical-olivo-cerebellar pathways project onto the corpus cerebella in three main longitudinal zones in the nonhuman primate (Zigmond *et al*, 1999).

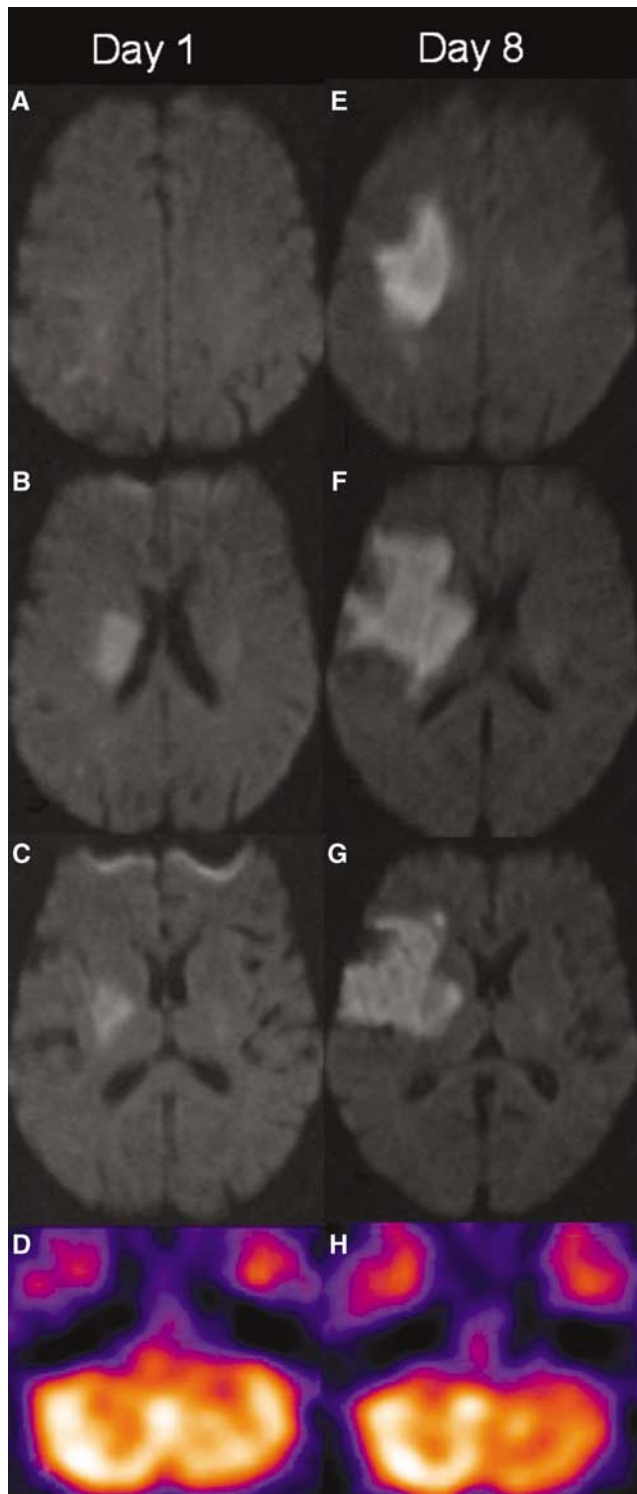


**Figure 2** A 73-year-old woman with left hemiparesis (Case 1). Six hours and twenty-five minutes after onset, the DWI images (A, B, and C) show ischemic lesion in the right basal ganglia, pyramidal tract in corona radiata, anterior limb, and genu of the internal capsule. A small lesion can also be seen in the supramarginal gyrus. Forty-five minutes after MRI, the SPECT image (D) shows mild hypoperfusion in the left cerebellar intermediate ( $AI = 1.5$ ) and lateral zones ( $AI = 5.7$ ). On day 8, the infarction extends to the lower part of the precentral gyrus, inferior frontal gyrus, anterior limb of internal capsule (E, F, and G), amygdale and entorhinal cortex (not provided) on DWI, and all the three cerebellar zones on the left show hypoperfusion on SPECT (AIs of medial, intermediate, and lateral zones = 7.2, 7.5, and 13.1, respectively) (H).

Including the fibers from spinal cord, the medial zone receives dorsal spinocerebellar tract, cuneocerebellar tract, and olivocerebellar tract. Besides the fiber tracts projecting to the medial zone, the intermediate zone also receives input from the cortico-ponto-cerebellar fibers that originate from

the motor cortex; the lateral zone receives olivocerebellar tract and pontocerebellar tract (Zigmond *et al*, 1999). Data of the detailed functional cerebrocerebellar connections in humans are still scanty.

Our results showed that the CCD significantly differed in the three zones. The AI of the medial zone was independently associated with DWI lesion locations in the temporal association cortex and the pyramidal tract in the corona radiata. However, only 2 of 22 patients (9%) presented with CCD within the first 48 h of stroke, supporting the assumption that the medial zone mainly receives spinocerebellar and cuneocerebellar information. The AI of the intermediate zone was independently associated with DWI lesion locations in motor cortices and the anterior part of the posterior limb of the internal capsule through which the pyramidal tract passes, suggesting that the intermediate zone receives mainly fiber projections from the pyramidal tract. The AI of the lateral zone was independently associated with DWI lesion locations in the motor cortices and the genu of the internal capsule through which the corticobulbar fibers pass.

In our study, the CCD was associated with DWI lesion volume and a number of cerebral areas and their fiber tracts in univariate analyses. Further stepwise multivariable linear regression analysis showed that within 48 h of onset, the AI of medial, intermediate, and lateral zones were each significantly associated with different DWI lesion locations. Although the CCD has been studied in stroke patients, the determinants of CCD remain controversial. Some determinants have been identified, such as lesions in the postcentral, supramarginal, and medial occipital regions (Komaba *et al*, 2004), anterior frontal lobe and anterior temporal lobe (Kamouchi *et al*, 2004), motor and premotor areas (Ishihara *et al*, 1999), frontoparietal lobes, basal ganglia and internal capsule (Kim *et al*, 1997), and volume (Infeld *et al*, 1995). Due to the different determinants for the three cerebellar zones, it is not surprising that the data on determinants in the previous studies are controversial, because the ROIs covering the whole hemisphere have been used to calculate the AI.

Our results also clarify the phenomenon that some patients do not have hemiparesis, but still have CCD

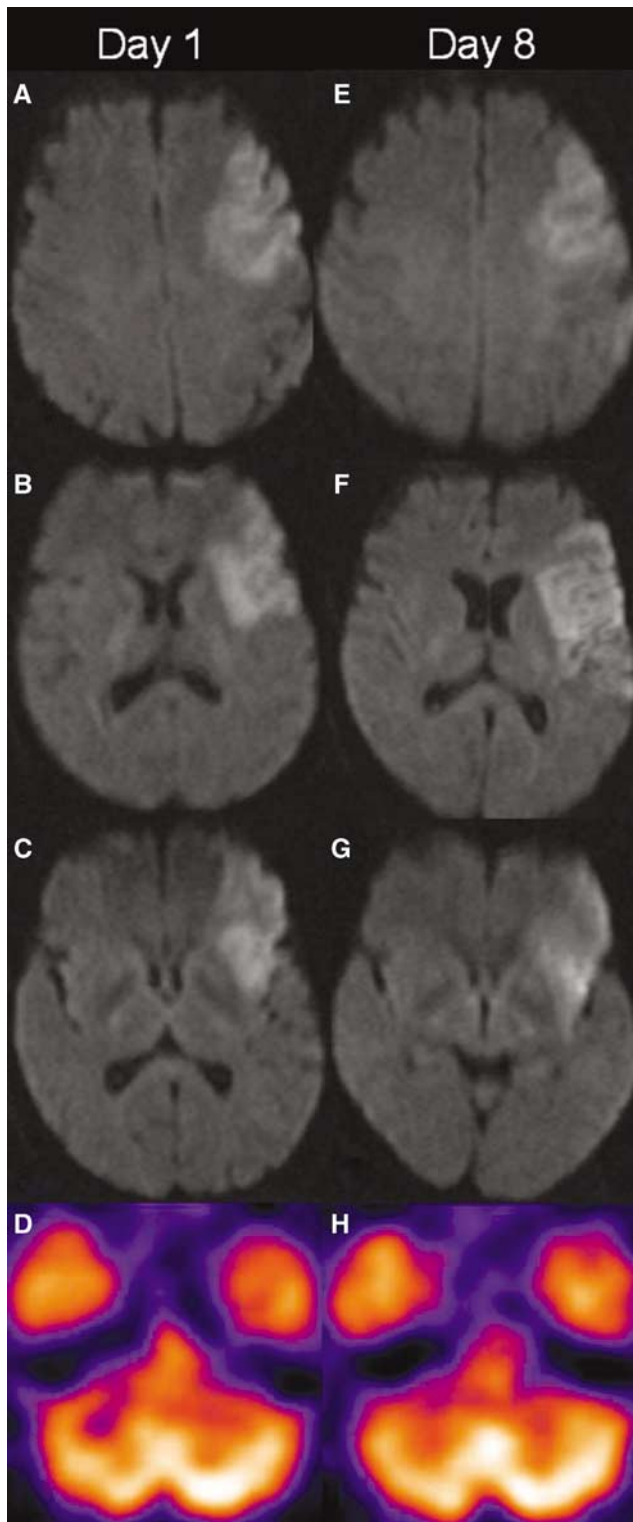


**Figure 3** A 53-year-old woman with right hemiparesis and aphasia (Case 13). Twenty-five and five minutes after onset, the DWI images (A, B, and C) show an ischemic lesion in the left precentral gyrus, inferior frontal gyrus, middle frontal gyrus, and orbitofrontal cortex. The SPECT image obtained at 26.6 h (D) shows hypoperfusion in the right cerebellar intermediate (AI = 2.9) and lateral zones (AI = 4.3). On day 8, although the infarction extended to the somatosensory and auditory cortex on DWI (E, F, and G), the extent and severity of hypoperfusion does not apparently change on SPECT (AIs of intermediate and lateral zones = 2.0 and 6.2, respectively) (H).

**Table 3** Correlation between clinical neurological status and cerebellar interhemispheric asymmetry index, and DWI lesion volumes

	Initial AI			Day 8 AI			DWI volume	
	Medial	Intermediate	Lateral	Medial	Intermediate	Lateral	Initial	Day 8
NIHSS Initial	0.537*	0.721**	0.798**	-0.128	0.509*	0.540**	0.685**	0.714**
NIHSS day 8	0.570**	0.619**	0.811**	0.105	0.596**	0.700**	0.731**	0.822**
NIHSS 3-Month	0.497*	0.451*	0.617**	0.036	0.604**	0.544*	0.528*	0.591**
MRS 3-Month	0.281	0.364	0.617**	-0.018	0.629**	0.620**	0.444*	0.550**

\* $P < 0.05$  and \*\* $P < 0.01$ . Pearson correlation coefficients were used.

(Pantano *et al*, 1986). The DWI lesion volumes were significantly associated with the AIs of the intermediate and lateral zones in univariate analyses, but the DWI lesion volume was excluded in the stepwise multivariable linear regression model. It seems that the infarction volume itself is not an independent determinant, but a large infarction is more likely to include important functional cortices and fiber pathways that contribute to CCD.

In our study, there was variable temporal evolution in CCD; because in some patients, the CCD vanished and in some patients, it increased during the first week, indicating perhaps also that irreversible damage might happen during the first week of stroke. In studies using animal models, CCD has been directly related to the loss of afferent stimuli from the supratentorial cortex, and has been a reversible functional phenomenon without structure change (Meyer *et al*, 1993). However, it has been shown that CCD caused by contralateral cerebral infarction might also cause irreversible damage (perhaps transneuronal degeneration) in the affected cerebellum. In a transient global ischemic rat model, the cerebellar Purkinje cells quickly died as a result of the pathological synaptic input from the inferior olive (Welsh *et al*, 2002). Six hours after MCA occlusion in a mouse model of stroke, increased immunoreactivity for biliverdin reductase, a sign of neuron damage, was found not only in the supratentorial ischemic core, but also in the Purkinje layer of the cerebellum (Panahian *et al*, 1999). Persistence of CCD could result in atrophy in the affected cerebellar hemisphere (Tien and Ashdown, 1992; Yamauchi *et al*, 1999). Single-photon emission computed tomography and PET studies in stroke patients support the theory that lack of CCD reversibility is probably due to functional deactivation and subsequent transneuronal degeneration (Kim and Lee, 2000; Pantano *et al*, 1986; Sobesky *et al*, 2005).

Interestingly the AI of the lateral zone within 48 h of onset, and the AI of the intermediate zone on day 8 were independently associated with the 3-month mRS. It has been reported in the literature that the CCD is related to poor neurological improvement after stroke (De Reuck *et al*, 1997; Sobesky *et al*, 2005; Takasawa *et al*, 2002). In our study, DWI lesions in the premotor and supplementary motor

cortex were the common determinants for the AIs of both intermediate and lateral zones, indicating that the network between the premotor and supplementary motor cortex, and cerebellum is important in the complex pathophysiology of stroke and CCD. Accumulative functional MRI data have shown that the premotor and supplementary motor cortex plays a crucial role in stroke recovery (Feydy *et al*, 2004; Loubinoux *et al*, 2003; Marshall *et al*, 2000). However, DWI lesion locations in the premotor and supplementary motor cortex were excluded as independent predictors of 3-month mRS in the multivariate analysis. The association between AIs and 3-month mRS may therefore not be a coincidence after damage in the premotor and supplementary motor cortex, and the CCD itself might be independently involved in stroke recovery. It is also interesting that besides the CCD, the parietal association cortex was also independently associated with the 3-month mRS. It has been well documented that the parietal association cortex is critically involved in multimodal proprioception, language comprehension, attention, and spatial awareness. The parietal association cortex might compensate for cerebellar function (Manto *et al*, 1999). An intact parietal association cortex is likely to be important in stroke recovery.

Using the AI to evaluate CCD might cause bias in a longitudinal study. It has been shown that a supratentorial stroke or functional ablation is associated with a decrease in spontaneous activity on the contralateral healthy hemisphere (transhemispheric diaschisis) (Enager *et al*, 2004; Witte *et al*, 2000), which can also project to the ipsilateral cerebellar hemisphere and result in a hemodynamic change. The AI may thus change as a function of recovery on the healthy side.

In conclusion, acute CCD is a result of functional deafference, while in the subacute phase, transneuronal degeneration might contribute to the CCD. The three cerebellar longitudinal zones receive common fibers, but also specific fibers via the cortico-ponto-cerebellar and cortical-olivo-cerebellar pathways. Loss of afferent stimulations from the primary, premotor, and supplementary motor cortices, primary somatosensory cortex, and temporal association cortex are related to the CCD of these individual zones.

## References

- Allen GI, Tsukahara N (1974) Cerebrocerebellar communication systems. *Physiol Rev* 54:957–1006
- Baron JC, Boussier MG, Comar D, Castaigne P (1980) Crossed cerebellar diaschisis in human supratentorial infarction. *Trans Am Neurol Assoc* 105:459–61
- Brodal A (1972) Cerebrocerebellar pathways. Anatomical data and some functional implications. *Acta Neurol Scand Suppl* 51:153–95
- De Reuck J, Decoo D, Lemahieu I, Striickmans K, Goethals P, Van Maele G (1997) Crossed cerebellar diaschisis after middle cerebral artery infarction. *Clin Neurol Neurosurg* 99:11–6
- Duvernoy HM (1991) *The human brain: surface, three-dimensional sectional anatomy and MRI*. Wien: Springer-Verlag
- Enager P, Gold L, Lauritzen M (2004) Impaired neurovascular coupling by transhemispheric diaschisis in rat cerebral cortex. *J Cereb Blood Flow Metab* 24:713–9
- Feeney DM, Baron JC (1986) Diaschisis. *Stroke* 17:817–30
- Feydy A, Krainik A, Bussel B, Maier MA (2004) Cortical reorganization allows for motor recovery after crossed cerebrocerebellar atrophy. *J Neuroimaging* 14:49–53
- Gold L, Lauritzen M (2002) Neuronal deactivation explains decreased cerebellar blood flow in response to focal cerebral ischemia or suppressed neocortical function. *Proc Natl Acad Sci USA* 99:7699–704
- Infeld B, Davis SM, Lichtenstein M, Mitchell PJ, Hopper JL (1995) Crossed cerebellar diaschisis and brain recovery after stroke. *Stroke* 26:90–5
- Ishihara M, Kumita S, Mizumura S, Kumazaki T (1999) Crossed cerebellar diaschisis: the role of motor and premotor areas in functional connections. *J Neuroimaging* 9:30–3
- Kamouchi M, Fujishima M, Saku Y, Ibayashi S, Iida M (2004) Crossed cerebellar hypoperfusion in hyperacute ischemic stroke. *J Neurol Sci* 225:65–9
- Kim SE, Choi CW, Yoon BW, Chung JK, Roh JH, Lee MC, Koh CS (1997) Crossed-cerebellar diaschisis in cerebral infarction: technetium-99m-HMPAO SPECT and MRI. *J Nucl Med* 38:14–9
- Kim SE, Lee MC (2000) Cerebellar vasoreactivity in stroke patients with crossed cerebellar diaschisis assessed by acetazolamide and 99mTc-HMPAO SPECT. *J Nucl Med* 41:416–20
- Komaba Y, Mishina M, Utsumi K, Katayama Y, Kobayashi S, Mori O (2004) Crossed cerebellar diaschisis in patients with cortical infarction: logistic regression analysis to control for confounding effects. *Stroke* 35:472–6
- Loubinoux I, Carel C, Pariente J, Dechaumont S, Albucher JF, Marque P, Manelfe C, Chollet F (2003) Correlation between cerebral reorganization and motor recovery after subcortical infarcts. *Neuroimage* 20:2166–80
- Manto M, Setta F, Jacquy J, Godaux E (1999) Cerebellar decompensation following a stroke in contralateral posterior parietal cortex. *J Neurol Sci* 167:117–20
- Marshall RS, Perera GM, Lazar RM, Krakauer JW, Constantine RC, DeLaPaz RL (2000) Evolution of cortical activation during recovery from corticospinal tract infarction. *Stroke* 31:656–61
- Meyer JS, Obara K, Muramatsu K (1993) Diaschisis. *Neurol Res* 15:362–6
- Moseley ME, Kucharczyk J, Mintorovitch J, Cohen Y, Kurhanewicz J, Derugin N, Asgari H, Norman D (1990) Diffusion-weighted MR imaging of acute stroke: correlation with T2-weighted and magnetic susceptibility-enhanced MR imaging in cats. *AJNR Am J Neuroradiol* 11:423–9
- Panahian N, Huang T, Maines MD (1999) Enhanced neuronal expression of the oxidoreductase–biliverdin reductase—after permanent focal cerebral ischemia. *Brain Res* 850:1–13
- Pantano P, Baron JC, Samson Y, Boussier MG, Derouesne C, Comar D (1986) Crossed cerebellar diaschisis. Further studies. *Brain* 109:677–94
- Schmahmann JD, Pandya DN (1997) The cerebrocerebellar system. *Int Rev Neurobiol* 41:31–60
- Sobesky J, Thiel A, Ghaemi M, Hilker RH, Rudolf J, Jacobs AH, Herholz K, Heiss WD (2005) Crossed cerebellar diaschisis in acute human stroke: a PET study of serial changes and response to supratentorial reperfusion. *J Cereb Blood Flow Metab* 25:1685–91
- Takasawa M, Watanabe M, Yamamoto S, Hoshi T, Sasaki T, Hashikawa K, Matsumoto M, Kinoshita N (2002) Prognostic value of subacute crossed cerebellar diaschisis: single-photon emission CT study in patients with middle cerebral artery territory infarct. *AJNR Am J Neuroradiol* 23:189–93
- Tien RD, Ashdown BC (1992) Crossed cerebellar diaschisis and crossed cerebellar atrophy: correlation of MR findings, clinical symptoms, and supratentorial diseases in 26 patients. *AJR Am J Roentgenol* 158:1155–9
- Welsh JP, Yuen G, Placantonakis DG, Vu TQ, Haiss F, O'Hearn E, Molliver ME, Aicher SA (2002) Why do Purkinje cells die so easily after global brain ischemia? Aldolase C, EAAT4, and the cerebellar contribution to posthypoxic myoclonus. *Adv Neurol* 89:331–59
- Witte OW, Bidmon HJ, Schiene K, Redecker C, Hagemann G (2000) Functional differentiation of multiple perilesional zones after focal cerebral ischemia. *J Cereb Blood Flow Metab* 20:1149–65
- Yamauchi H, Fukuyama H, Nagahama Y, Nishizawa S, Konishi J (1999) Uncoupling of oxygen and glucose metabolism in persistent crossed cerebellar diaschisis. *Stroke* 30:1424–8
- Zigmond MJ, Bloom FE, Landis SC, Roberts JL, Squir LR (1999) *Fundamental neuroscience*. San Diego, CA: Academic Press